Progress in Energy and Environment

Journal homepage: https://www.akademiabaru.com/submit/index.php/progee
Link to this article: https://doi.org/10.37934/progee.24.1.110

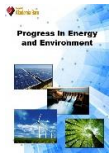

Volume 24 (2023) 1-10

Original Article

Iron oxide nanoparticles derived from *Chlorella vulgaris* extract: Characterization and crystal violet photodegradation studies

OPEN ACCESS

Peck Loo Kiew[*,1], Nur Ainaa[1], Shania[1], Lam Man Kee[2], Tan Lian See[1], Yeoh Wei Ming[3]

[1] Department of Chemical and Environmental Engineering, Malaysia - Japan International Institute of Technology, Universiti Teknologi Malaysia, Jalan Sultan Yahya Petra, 54100 Kuala Lumpur, Malaysia
[2] Department of Chemical Engineering, HICoE-Centre for Biofuel and Biochemical Research, Institute of Self-Sustainable Building, University Teknologi PETRONAS, 32610, Seri Iskandar, Perak, Malaysia
[3] Department of Petrochemical Engineering, Universiti Tunku Abdul Rahman, 31900 Kampar, Perak, Malaysia
[*] **Correspondence email:** plkiew@utm.my

Abstract

Nanoparticles were first used a century ago, but have recently gained popularity due to their ease of use, eco-friendliness, pollution-free nature, nontoxicity and low cost for wastewater treatment applications. In terms of nanoparticles preparation, green synthesis is a more convenient, economical, quick, and environmentally friendly process than traditional synthesis (i.e. chemical and mechanical) methods. The objective of this study was to synthesise iron oxide nanoparticles from iron (III) chloride using microalgae (*Chlorella vulgaris*) extract for photodegradation of crystal violet (CV) dye. Various characterization methods such as X-ray diffraction (XRD), field emission scanning electron microscopy (FESEM), and Fourier-transform infrared spectroscopy (FTIR) were used to examine properties of the nanoparticles including its crystallinity, morphologies and sizes, and functional groups, respectively. The CV photodegradation process was carried out under different process conditions included initial CV concentration (10 mg/L – 25 mg/L), CV solution pH (5.39 – 8.98), and irradiation period (30 – 90 mins) to investigate the optimum operating conditions for the CV removal. The analysis using FESEM demonstrated that the nanoparticles exhibited irregularities and cylindrical shapes, measuring 109 nm in size. Meanwhile, the XRD analysis indicated that the iron oxide nanoparticles possessed a tetragonal crystal structure. The presence of Fe-O stretching vibrations at 486 cm^{-1} was confirmed by the FTIR spectrum. In terms of CV photodegradation studies, the optimum operating conditions for CV removal using iron oxide nanoparticles were determined to be at initial CV concentration of 10 mg/L, solution pH of 8.98, and an irradiation period of 90 mins, with a percentage removal of 96.21 %.

Article Info

Received 2 January 2023
Received in revised from 18 March 2023
Accepted 20 March 2023
Available online 27 March 2023

Keywords

Crystal violet
Iron oxide nanoparticle
Photodegradation
Microalgae
Extract

1 Introduction

Textile, paint and varnish, ink, plastics, pulp and paper, cosmetics and tanneries, as well as dye-producing firms, all generate considerable amounts of wastewater that contains dyes as a significant component of the waste stream. Colored dye effluents endanger local ecosystems. Colors can be extremely toxic and dangerous in many cases. With a wide range of applications, crystal violet (CV) has become a well-known dye. It can be used for everything from skin care and cosmetics to animal medicine and poultry feed additives that help prevent mold and fungal growth, among other things. In

addition, it is frequently used in textile dyeing and printing processes. CV dye is toxic and mutagenic at the same time. Adsorption [1], photodegradation, coagulation flocculation, chemical oxidation [2], electrochemical oxidation [3], and biological processes are just some of the treatment methods available to remove dye pollutants from wastewater [4]. The above-mentioned methods for removing dyes from wastewater have several limitations, primarily a low removal effectiveness [5], because dyes are light and oxidizing agent stable [6]. Heterogeneous photocatalysis [7] is a potential alternative to all the methods because it is an advanced oxidation technology that allows for the removal of a wide range of organic pollutants at a high rate of degradation [8]. It is superior to other treatment methods because it could be operated in all weather conditions of mild pressure and temperature, as well as at very low pollutant concentrations. This process employs ultraviolet (UV) radiation and an oxidizing chemical to create hydroxyl radicals. These radicals then non-selectively target organic molecules during the photodegradation process.

Numerous studies have been published on the use of nanoparticles for dye removal from wastewater using photodegradation, including titanium dioxide [9], gold [9], and iron oxide nanoparticles [10]. Nathan et al. [11] discovered that iron (III) oxide nanoparticles (Fe_2O_3-NPs) synthesised using *Rhizophora mucronate Lam* demonstrated remarkable photodegradation efficiency, lowering phenol red and CV by 83% and 95%, respectively, when exposed to fluorescent light. Titanium dioxide nanoparticles have also been shown to photodegrade CV dye up to 98 % after 25 mins of UV light exposure [12]. As a result, nanomaterials have been regarded as efficient, cost-effective, and environmentally friendly wastewater treatment materials, particularly for heavy metal and dye removal, as an adsorbent and photocatalyst for pollutant degradation.

Green production of microalgae-based silver nanoparticles is becoming more popular due to their antimicrobial properties. However, reports on the synthesis of other metallic microalgae-based nanoparticles, such as iron oxide, are scarce. Furthermore, the use of microalgae-based nanoparticles for CV removal via photocatalytic degradation remains unexplored. In this study, the potential of producing iron oxide nanoparticles using *Chlorella vulgaris* extract is explored. Various characterization methods are used to examine the physical properties and functional groups of the nanoparticles produced. The ability of iron oxide nanoparticles derived from *C. vulgaris* to photodegrade CV dye in the presence of UV light is studied in relation to various process parameters such as initial CV dye concentration, solution pH, and UV irradiation period.

2 Methodology and Experimental Set-Up

2.1 Synthesis of iron oxide nanoparticles from C. vulgaris extract

The iron oxide nanoparticles were synthesized following the procedures reported by Mishra et al. [13] with slight modifications. Briefly, 40 mL of *C. vulgaris* extract was added to 360 mL of 0.1 M iron (III) chloride solutions. After 2 hours of stirring at 70 °C, the solution changed colour to dark brown, suggesting the production of the iron oxide nanoparticles. Centrifugation at 10, 000 rpm and 25 °C for approximately 30 mins was then done to isolate the nanoparticles. This procedure was repeated twice to remove any biomaterials from the surfaces of the nanoparticles. The nanoparticles were dried and stored in an airtight container for future use.

2.2 Characterization of iron oxide nanoparticles

Various analysis were employed to characterize the iron oxide nanoparticles that were synthesized whereby X-ray diffraction (XRD) analysis was done using Cu-Kα radiation (k = 1.54 Å) at 45 kV and 40 mA. Meanwhile, the shape and morphology of the nanoparticles were determined by field emission scanning electron microscopy (FESEM). The presence of functional groups in synthesized iron oxide nanoparticles is investigated using Fourier-transform infrared spectroscopy (FTIR) in the wavelength range 400-4000 cm^{-1}.

2.3 Photodegradation of crystal violet using iron oxide nanoparticles

UV light irradiation was used to investigate the photodegradation efficacy of the synthesised iron oxide nanoparticles for CV degradation. 50 mg of the iron oxide nanoparticles were added to 100 mL of CV solution with an initial concentration of 10 mg/L. A UV light (with wavelength of 395 nm) was used as

the source of the irradiation. The mixture was agitated in the presence of UV light for 30, 50, 70, and 90 mins to determine the CV removal percentage. The concentration of the CV dye solution after the irradiation was measured using a UV-Vis spectrophotometer at a wavelength of 582 nm. The CV removal percentage removal was calculated using Eq. (1):

$$\text{Percentage removal (\%)} = \frac{C_0 - C_t}{C_0} \times 100\% \quad (1)$$

where C_o and C_t was the concentration of CV in the solution before and after irradiation, respectively. C_t was calculated based on the correlation (obtained from calibration curve) presented in Eq. (2):

$$y = 0.1108x \text{ , } R^2 = 0.9964 \quad (2)$$

where y was the absorbance value measured at 582 nm and x was the concentration of CV dye (mg/L).

2.4 Removal of crystal violet using iron oxide nanoparticles without UV irradiation

To reveal the photodegradation ability of iron nanoparticles on the CV dye, the same procedures as described in Section 2.3 were repeated without UV irradiation. 100 mL of CV solution with an initial concentration of 10 mg/L was mixed with 50 mg of iron oxide nanoparticles, and stirring was conducted for 30, 50, 70, and 90 mins in the absence of UV irradiation. The purpose of this was to determine the percentage of CV removed from the solution by the adsorption process in the absence of UV irradiation and to confirm the removal of CV dye through photodegradation. Table 1 shows the process parameters for comparing CV adsorption and photodegradation in this study.

Table 1 The process parameters fixed for CV removal in this study.

Parameter	Unit	Value
Initial CV concentration	mg/L	10
Iron Oxide Nanoparticles	mg	50
Volume of CV Solution	mL	100
Irradiation Period	mins	30, 50,70 and 90

2.5 Effect of different parameters on photodegradation process

A few parameters were manipulated throughout the photodegradation process to optimise the CV degradation. These included initial CV dye concentration, solution pH, and irradiation period.

2.5.1 Effect of initial CV dye concentration

To determine the effect of the initial CV concentration on the photodegradation performance of iron oxide nanoparticles, the concentration was varied between 10, 15, 20, and 25 mg/L while all other experimental parameters remained constant. The pH of the solution was kept at 8, while the radiation temperature and time were maintained at 25 °C and 90 mins, respectively. The percentage of CV removal was then calculated using Eq. (1) for each initial concentration investigated.

2.5.2 Effect of solution pH

The influence of pH on CV photodegradation was investigated by varying the pH of the CV solution. 0.05 M hydrochloric acid (HCl) and 0.05 M sodium hydroxide (NaOH) solution were used to change the pH of the solution. The pH of the CV solution was adjusted to 5.39, 6.07, 7.68, and 8.98. After that, the photodegradation experiments were carried out for 90 mins at 25 °C using the optimum initial CV dye concentration determined in Section 2.5.1. The CV percentage removal was then calculated using Eq. (1) for each pH tested.

2.5.3 Effect of irradiation period

The effect of different irradiation period was studied with the photodegradation experiments conducted for 30, 50, 70 and 90 mins, at the optimum initial CV concentration and solution pH determined in Section 2.4.1 and 2.4.2, respectively. The CV percentage removal was then calculated using Eq. (1) for each irradiation period investigated.

3 Results and Discussion

3.1 Characterization of iron oxide nanoparticles

In this study, the production of iron oxide nanoparticles involved mixing the solution of iron (III) chloride with *C. vulgaris* extract, which acted as a reducing agent. The color of the solution changed to a dark brown, indicating the formation of iron oxide nanoparticles. This change was attributed to the surface plasmon excitation in the iron-associated nanoparticles [14].

3.1.1 X-Ray Diffraction (XRD)

Characterization of iron oxide nanoparticles was performed in this study using the XRD pattern by determining the width of the peaks in the XRD pattern. The XRD spectrum of the synthesised iron oxide nanoparticles is shown in Fig. 1. The XRD pattern shows diffraction peaks at 11.96°, 16.88 °, 26.81 °, 34.04 °, 35.29 °, 39.33 °, 46.53 °, 52.02 ° and 55.95 ° marked by their indices (1 1 0), (0 2 0), (1 3 0), (2 1 1), and (6 2 0) respectively. The results obtained were almost identical to the peaks of gamma-Fe_2O_3 crystal with the tetragonal structure when compared with *ICDD data* card no. *00-034-1266*. The results are in agreement with the standard XRD pattern of gamma-Fe_2O_3 [15]. Hence, it was clear that iron oxide nanoparticles formed using *C. vulgaris* were crystalline in nature.

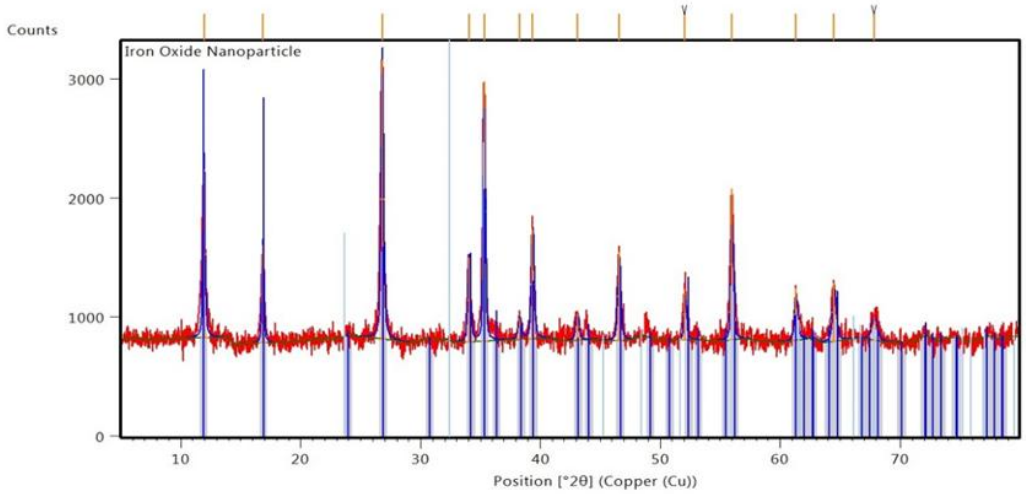

Fig. 1 XRD spectrum of iron oxide nanoparticles.

3.1.2 Field Emission Scanning Electron Microscopy (FESEM)

Fig. 2 shows FESEM images of the synthesised iron oxide nanoparticles, which revealed a sphere with cylindrical shape and a size of about 109 nm. Zheng et al. [16] discovered similar results when synthesising iron oxide nanoparticles which were also cylindrical in shape. In addition, the iron oxide nanoparticle composition was determined using energy dispersive X-Ray (EDX), as shown in Fig. 3. The highest peaks on the EDX graph were found to be the components Fe and O, which were the expected iron oxide nanoparticles.

3.1.3 Fourier-Transform Infrared Spectroscopy (FTIR)

The presence of any functional group on the surface of nanoparticles was detected using FTIR analysis. The FTIR spectrum of the iron oxide nanoparticles produced is shown in Fig. 4. The FTIR spectrum exhibits several distinguishing peaks whereby the peak at 3433 cm^{-1} was attributed to the OH group's O-H stretching [17]. Peak 1636 cm^{-1} represented the stretching vibration band of C=C bonds [18]. The stretch group C-O-C and =C-H were represented at bands of 1061 cm^{-1} and 850 cm^{-1}, respectively [19]. The detected peak at 682 cm^{-1} belonged to the metal-oxygen group [19], whereas the peak at 486 cm^{-1} corresponded to the Fe-O stretching vibrations, which confirmed the formation of iron oxide nanoparticles [21].

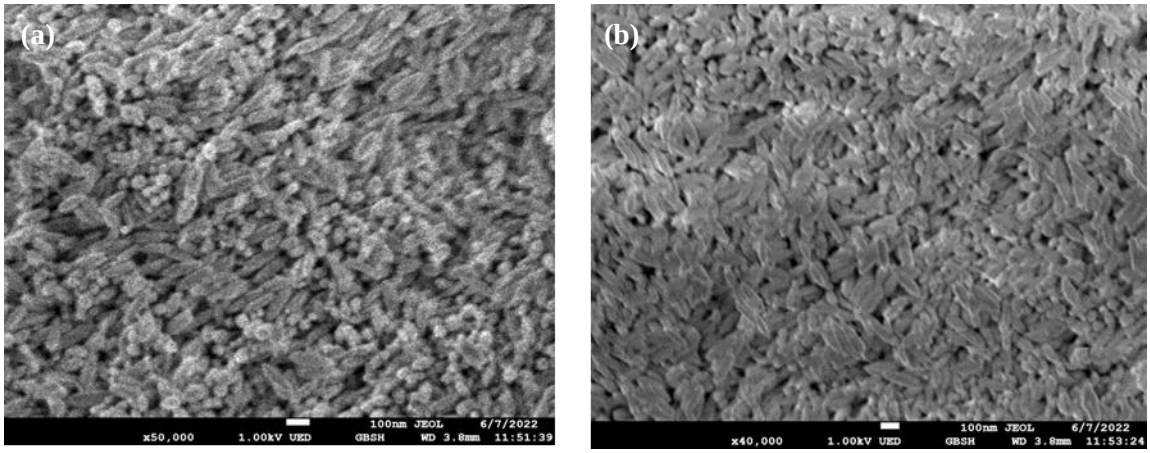

Fig. 2 FESEM image of the synthesized iron oxide nanoparticles at (a) magnification of x50k and (b) magnification of x40k

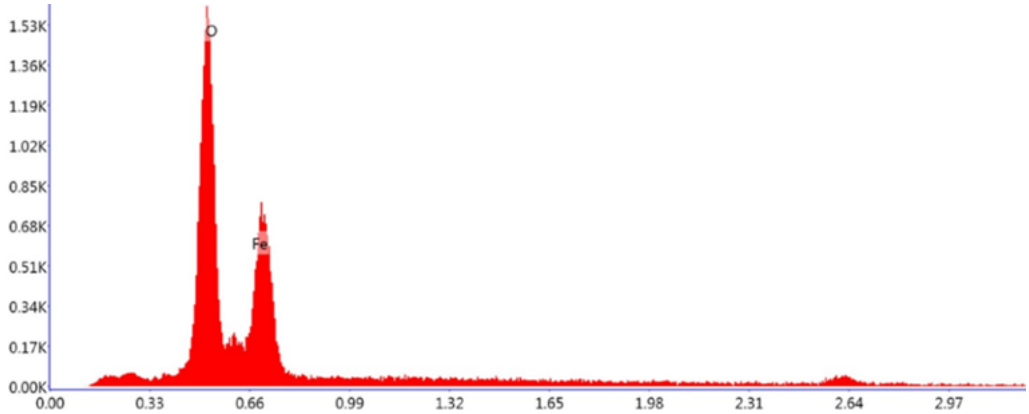

Fig. 3 EDX graph of the synthesized iron oxide nanoparticles

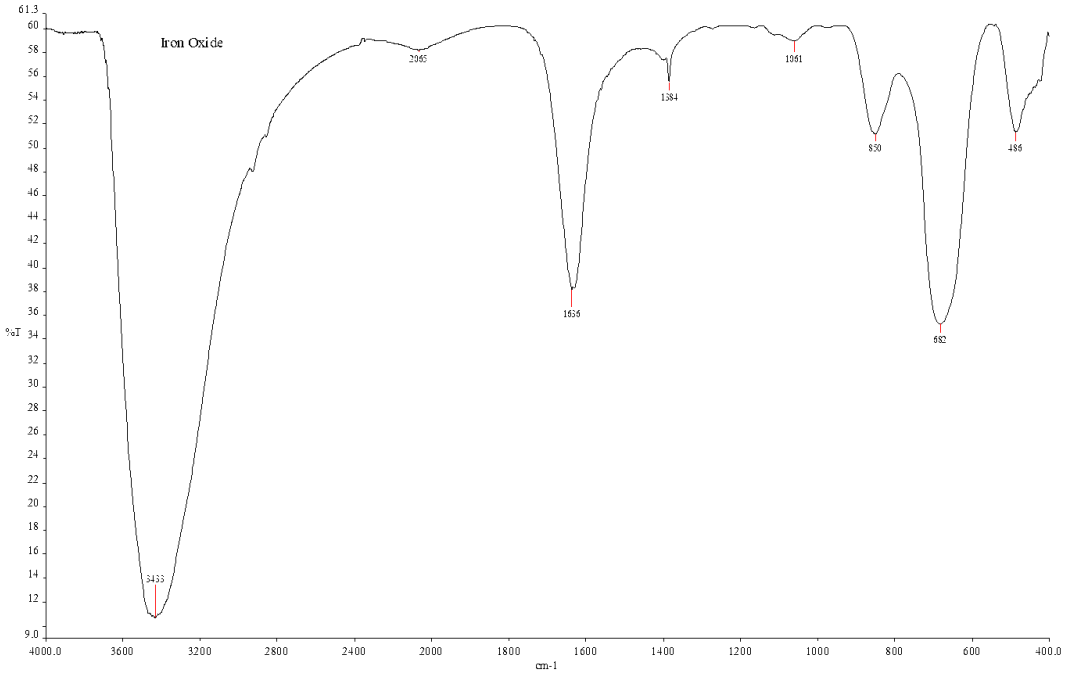

Fig. 4 FTIR spectrum of synthesized iron oxide nanoparticles.

3.2 Photodegradation of crystal violet using iron oxide nanoparticles

Iron oxide nanoparticles were investigated for their ability to photodegrade CV dye. The dye removal process was carried out in two conditions namely with the presence of UV light and in the dark (without UV irradiation). The experiment was carried out in the dark to determine whether an adsorption process was taking place. The colour of the solution changed from purple to nearly colourless as CV dye was removed from the solution.

Fig. 5 depicts the percentages of CV removal when stirring iron oxide nanoparticles in the dark and in the presence of UV light for 90 mins. The percentage removal differed significantly between the two conditions, with a higher removal percentage consistently recorded under the UV lamp for all tested periods compared to those in the dark. These findings indicated that the synthesised iron nanoparticles could be used as an adsorbent in the absence of UV light and could potentially be investigated for their ability to photodegrade CV. According to Bhuiyan et al. [10], UV light irradiation caused the iron oxide nanoparticles to form hydroxyl radicals, which resulted in the formation of a hole (h^+) and electron (e^-) pair. This hole would convert water into a hydroxyl radical, causing the dye to oxidise and degrade. At the same time, when the electron combined with an oxygen molecule, it formed a superoxide radical, which was then transformed into a powerful oxidising agent, the hydroxyl radical, which would then break down the dye into harmless by-products.

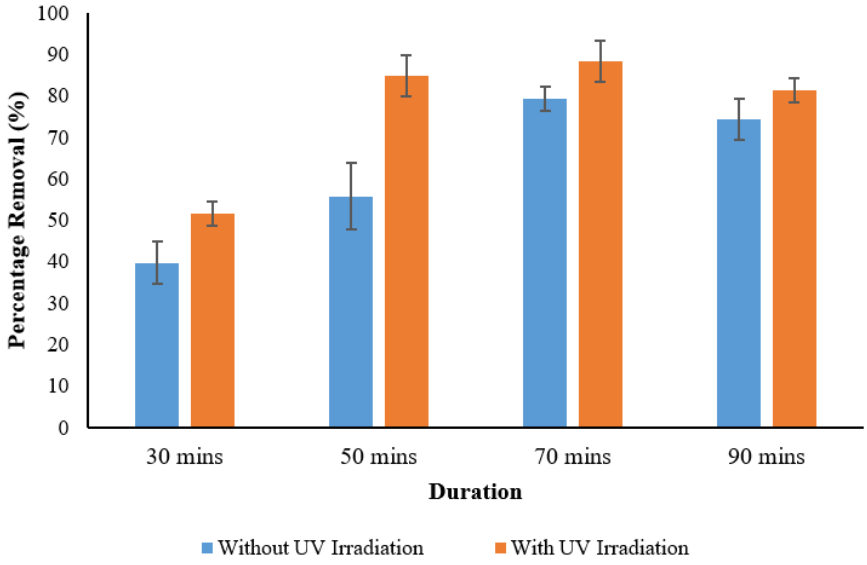

Fig. 5 The effect of irradiation time on the percentage removal of CV in the dark and under the UV lamp.

The initial 70 mins showed a rapid removal of CV dye. Following that, a slightly lower removal percentage was observed, which is possibly due to the desorption of CV dye from the nanoparticle surface. However, to reinforce this desorption hypothesis, further studies are required to measure the pH of the CV dye solution along the removal process. Notably, the performance of iron oxide nanoparticles in removing CV dye in the presence of UV light was significantly superior to that in the dark, despite the similar percentage removal trend.

3.3 Optimization of crystal violet photodegradation process

3.3.1 Effect of initial concentration of crystal violet

Initial dye concentration is a powerful driving force in overcoming the mass transfer resistance of molecules between the aqueous and solid phases in wastewater treatment processes. To assess the influence of initial CV concentration on photodegradation, the concentration was varied from 10 mg/L to 25 mg/L. The graph in Fig. 6 depicts the experimental results for the percentage removal of CV with varying initial CV concentrations.

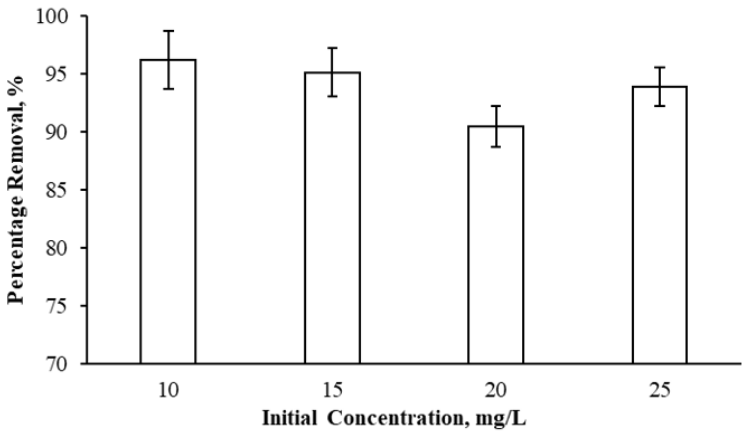

Fig. 6 The effect of initial concentration on the CV removal percentage.

It was discovered that as the initial concentration of CV increased, the removal of CV decreased, demonstrating that the degradation efficiency and initial concentration of the dyes were inversely proportional to one another. This result was consistent with the findings by Talib and Al-Kadum [21] who discovered that increasing the initial CV dye concentration from 1 x 10^{-5} M to 5 x 10^{-5} M in the presence of UV irradiation reduced the percentage of CV dye removal from 42.3 % to 16%. According to Piranshahi et al. [12], when the CV initial concentration was increased, photons were intercepted before they could reach the surface of the iron oxide nanoparticles, resulting in a decrease in photon absorption by the nanoparticles, hence reducing the photodegradation efficiency. Jouali et al. [22] explained that at high initial concentrations, the dye molecules prevented UV light from reaching the photocatalyst (iron oxide nanoparticles in this study), reducing the amount of hydroxyl radicals formed. Furthermore, because the amount of iron oxide nanoparticles was constant, the decrease in photodegradation efficiency as the initial CV concentration was increased in this study could be attributed to an insufficient number of free radicals to break down the dye. Although there was a slight increase in the percentage of CV removal when the initial concentration of CV was raised to 25 mg/L, the result was not significantly different from that of the initial concentration of 20 mg/L.

3.3.2 Effect of pH of the solution

pH of the solution affects both the surface charge of the nanoparticles and the CV dye. The electrostatic interactions of nanoparticle surfaces with other substances, such as solvent molecules, substrate molecules, and charged radicals produced during photodegradation, are highly pH dependent. In this study, the effect of pH on CV photodegradation was investigated over a pH range of 5.39 to 8.98 for an initial dye concentration of 10 mg/L and an irradiation period of 90 mins. Fig. 7 shows the results of CV removal percentage as the pH of the solution was changed.

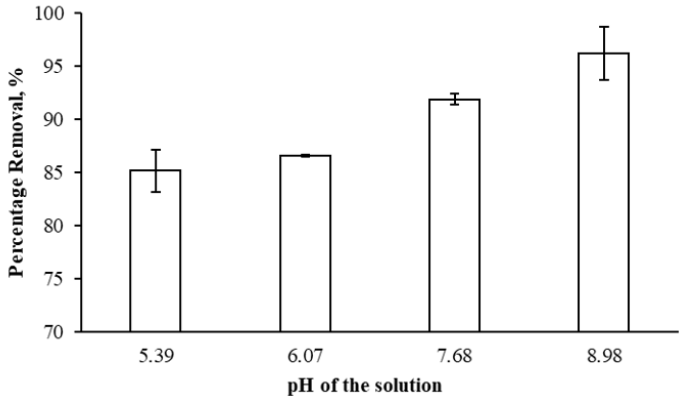

Fig. 7 The effect of pH on the CV removal percentage.

The results showed that pH 8.98 demonstrated the highest CV removal percentage from the solution (96.21%), while pH 5.29 resulted in the lowest removal percentage (85%). As shown in Fig. 7, increasing the pH from 5.39 to 8.98 significantly improved the elimination of CV dye from the aqueous solution. According to the literature, the rate of CV photodegradation typically increases as pH rises [23,24]. The photocatalyst, iron oxide nanoparticles with negative charges, became more accessible to the cationic CV dye molecules in the solution as the pH increased from 5.39 to 8.98, allowing for the formation of more hydroxyl radicals.

3.3.3 Effect of irradiation period

Several UV light irradiation periods ranging from 30 to 90 mins were investigated to determine the photodegradation effectiveness of CV using iron oxide nanoparticles (Fig. 8). The results showed positive correlation between the irradiation period with the CV removal percentage. The highest CV removal was 96.21 % after 90 mins of irradiation time, whereas the lowest percentage removal was 51.62 % at 30 mins. Wardhani et al. [24] explained that the amount of time exposed to UV radiation was proportional to the percentage elimination of CV dye. As more hydroxyl radicals were produced, the photodegradation efficiency increased until it reached an equilibrium level. According to Abdullah et al. [25], during the photodegradation process, the irradiation time is defined as the time when the iron oxide nanoparticles interact with the inner rays to produce hydroxyl radicals, as well as the time when the hydroxyl radicals interact with the organic component substrate. The CV compounds will be broken down by hydroxyl radicals, which are powerful oxidizers. As a result, the higher the amount of hydroxyl radicals produced, the higher the percentage of photodegradation attained. The results obtained in the present study was consistent with those of Kumar and Pandey [26], who attributed the observed trend to the interaction of dye molecules with the surface of the photocatalyst. As the irradiation time increased, so did the interaction of dye molecules with the surface of the photocatalyst. As a result, the photodegradation efficiency was enhanced.

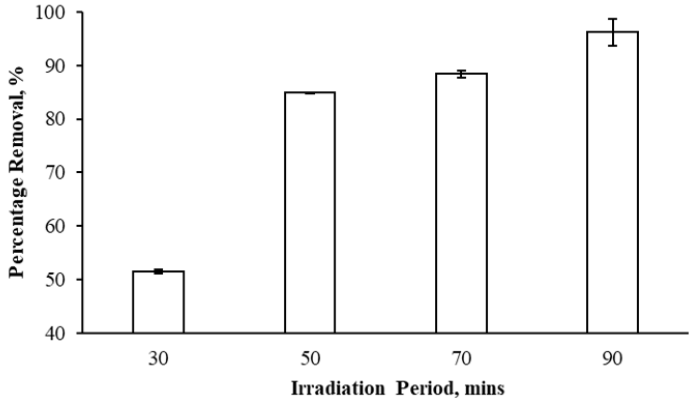

Fig. 8 Effect of irradiation period on percentage removal of CV.

4 Conclusion

Iron oxide nanoparticles synthesised from *C. vulgaris* extract were found to be a potential photocatalyst for CV dye photodegradation in this study. The characterization results of the nanoparticles revealed that the nanoparticles' properties were acceptable, though optimization of the synthesis procedures may be required to achieve particle sizes less than 100 nm. The experimental results revealed a significant difference in the percentage removal of CV dye from the solution when CV removal was performed in the dark versus under UV light, with the latter consistently resulting in higher CV removal percentage removal up to 90 mins. The highest CV removal percentage of 96.21 % could be achieved at the initial CV dye concentration of 10 mg/L, pH of 8.98 and 90 mins of irradiation period. The present study found that synthesising iron oxide nanoparticles from *C. vulgaris* extract and using them to photodegrade crystal violet dye was feasible. To further investigate the effectiveness of green iron oxide nanoparticles in removing CV dye from aqueous solution, detailed optimization of iron oxide nanoparticle synthesis or preparation is suggested.

Declaration of Conflict of Interest

The authors declared that there is no conflict of interest with any other party on the publication of the current work.

ORCID

Peck Loo Kiew https://orcid.org/0000-0001-5051-9909
Lian See Tan https://orcid.org/0000-0001-9039-7926
Yeoh Wei Ming https://orcid.org/0009-0009-4896-438X

Acknowledgement

This work is financially supported by Universiti Teknologi Malaysia, UTM Encouragement Research (UTMER) with Reference No. PY/2021/01231/ Q.K130000.3843.20J90.

References

[1] M.T. Yagub, T.K. Sen, S. Afroze, H.M. Ang, Dye and its removal from aqueous solution by adsorption: A review, in: Advances in Colloid and Interface Science, Elsevier, 2014: pp. 172–184. https://doi.org/10.1016/j.cis.2014.04.002.

[2] O. Türgay, G. Ersöz, S. Atalay, J. Forss, U. Welander, The treatment of azo dyes found in textile industry wastewater by anaerobic biological method and chemical oxidation, Separation and Purification Technology 79 (2011) 26–33. https://doi.org/10.1016/j.seppur.2011.03.007.

[3] S. Singh, S.L. Lo, V.C. Srivastava, A.D. Hiwarkar, Comparative study of electrochemical oxidation for dye degradation: Parametric optimization and mechanism identification, Journal of Environmental Chemical Engineering 4 (2016) 2911–2921. https://doi.org/10.1016/j.jece.2016.05.036.

[4] D. Bhatia, N.R. Sharma, J. Singh, R.S. Kanwar, Biological methods for textile dye removal from wastewater: A review, Critical Reviews in Environmental Science and Technology 47 (2017) 1836–1876. https://doi.org/10.1080/10643389.2017.1393263.

[5] A. Ghaffar, L. Zhang, X. Zhu, B. Chen, Porous PVdF/GO nanofibrous membranes for selective separation and recycling of charged organic dyes from water, Environmental Science and Technology 52 (2018) 4265–4274. https://doi.org/10.1021/acs.est.7b06081.

[6] R. Cristóvão, C. Botelho, R. Martins, R. Boaventura, Pollution prevention and wastewater treatment in fish canning industries of Northern Portugal, International Proceedings of Chemical, Biological and Environmental Engineering 32 (2012) 12–16. https://doi.org/10.7763/IPCBEE.

[7] O. Sacco, V. Vaiano, C. Han, D. Sannino, D.D. Dionysiou, Photocatalytic removal of atrazine using N-doped TiO_2 supported on phosphors, Applied Catalysis B: Environmental 164 (2015) 462–474. https://doi.org/10.1016/j.apcatb.2014.09.062.

[8] O. Sacco, V. Vaiano, L. Rizzo, D. Sannino, Photocatalytic activity of a visible light active structured photocatalyst developed for municipal wastewater treatment Journal of Cleaner Production. 175 (2018) 38–49. https://doi.org/10.1016/j.jclepro.2017.11.088.

[9] S.Y. Lee, D. Kang, S. Jeong, H.T. Do, J.H. Kim, Photocatalytic degradation of Rhodamine B dye by TiO_2 and gold nanoparticles supported on a floating porous polydimethylsiloxane sponge under ultraviolet and visible light irradiation, ACS Omega 5 (2020) 4233−4241. https://doi.org/10.1021/acsomega.9b04127.

[10] M.S.H. Bhuiyan, M.Y. Miah, S.C. Paul, T.D. Aka, O. Saha, M.M. Rahaman, J.I. Sharif, O. Habiba, M. Ashaduzzaman, Green synthesis of iron oxide nanoparticle using Carica papaya leaf extract: application for photocatalytic degradation of remazol yellow RR dye and antibacterial activity Heliyon. 6 (2020) e04603. https://doi.org/10.1016/j.heliyon.2020.e04603.

[11] V.K. Nathan, P. Ammini, J. Vijayan, Photocatalytic degradation of synthetic dyes using iron (III) oxide nanoparticles (Fe_2O_3-Nps) synthesised using *Rhizophora mucronata* Lam, IET Biotechnology 13 (2019) 120–123. https://doi.org/10.1049/iet-nbt.2018.5230.

[12] Z.A. Piranshahi, M. Behbahani, F. Zeraatpisheh, Synthesis, characterization and photocatalytic application of TiO_2/magnetic graphene for efficient photodegradation of crystal violet, Applied Organometallic Chemistry 32 (2017) e3985. https://doi.org/10.1002/aoc.3985.

[13] K. Mishra, N. Basavegowda, Y.R. Lee, Biosynthesis of Fe, Pd, and Fe-Pd bimetallic nanoparticles and their application as recyclable catalysts for [3 + 2] cycloaddition reaction: A comparative approach, Catalysis Science and Technology 5 (2015) 2612–2621. https://doi.org/10.1039/c5cy00099h.

[14] V. Gopinath, S. Priyadarshini, N. Meera Priyadharsshini, K. Pandian, P. Velusamy, Biogenic synthesis of antibacterial silver chloride nanoparticles using leaf extracts of *Cissus quadrangularis* Linn, Materials Letters 91 (2013) 224–227. https://doi.org/10.1016/j.matlet.2012.09.102.
[15] D. Mishra, R. Arora, S. Lahiri, S.S. Amritphale, N. Chandra, Synthesis and characterization of iron oxide nanoparticles by solvothermal method, Protection of Metals and Physical Chemistry of Surfaces 50 (2014) 628–631. https://doi.org/10.1134/S2070205114050128.
[16] X. Zheng, Y. Jiao, F. Chai, F. Qu, A. Umar, X. Wu, Template-free growth of well-crystalline α-Fe_2O_3 nanopeanuts with enhanced visible-light driven photocatalytic properties, Journal of Colloid and Interface Science 457 (2015) 345–352. https://doi.org/10.1016/j.jcis.2015.07.023.
[17] M. Jamzad, M. Kamari Bidkorpeh, Green synthesis of iron oxide nanoparticles by the aqueous extract of *Laurus nobilis* L. leaves and evaluation of the antimicrobial activity, Journal of Nanostructure in Chemistry 10 (2020) 193–201. https://doi.org/10.1007/s40097-020-00341-1.
[18] H. Veisi, L. Mohammadi, S. Hemmati, T. Tamoradi, P. Mohammadi, In situ immobilized silver nanoparticles on Rubia tinctorum extract-coated ultrasmall iron oxide nanoparticles: An efficient nanocatalyst with magnetic recyclability for synthesis of propargylamines by A^3 coupling reaction, ACS Omega 4 (2019) 13991–14003. https://doi.org/10.1021/acsomega.9b01720.
[19] S.M. Shalaby, F.F. Madkour, H.Y. El-Kassas, A.A. Mohamed, A.M. Elgarahy, Green synthesis of recyclable iron oxide nanoparticles using *Spirulina platensis* microalgae for adsorptive removal of cationic and anionic dyes, Environmental Science and Pollution Research 28 (2021) 65549–65572. https://doi.org/10.1007/s11356-021-15544-4.
[20] M.V. Arularasu, J. Devakumar, T.V. Rajendran, An innovative approach for green synthesis of iron oxide nanoparticles: Characterization and its photocatalytic activity, Polyhedron 156 (2018) 279–290. https://doi.org/10.1016/j.poly.2018.09.036.
[21] Z. Talib, A. Al-Kadum, Optimization of degradation crystal violet utilizing photocatalyst ZnO/UV Light, Journal University of Kerbala 16 (2018) 10–19.
[22] A. Jouali, A. Salhi, A. Aguedach, A. Aarfane, H. Ghazzaf, E.K. Lhadi, M. el Krati, S. Tahiri, Photo-catalytic degradation of methylene blue and reactive blue 21 dyes in dynamic mode using TiO_2 particles immobilized on cellulosic fibers, Journal of Photochemistry and Photobiology A: Chemistry 383 (2019). https://doi.org/10.1016/j.jphotochem.2019.112013.
[23] K.M. Reza, A. Kurny, F. Gulshan, Parameters affecting the photocatalytic degradation of dyes using TiO_2: A review, Applied Water Science 7 (2017) 1569–1578. https://doi.org/10.1007/s13201-015-0367-y.
[24] S. Wardhani, D. Purwonugroho, C.W. Fitri, Y.P. Prananto, Effect of pH and irradiation time on TiO_2-chitosan activity for phenol photo-degradation, AIP Conference Proceedings 2021 (2018) 1–7. https://doi.org/10.1063/1.5062759.
[25] A.M. Abdullah, N.J. Al-Thani, K. Tawbi, H. Al-Kandari, Carbon/nitrogen-doped TiO_2: New synthesis route, characterization and application for phenol degradation, Arabian Journal of Chemistry 9 (2016) 229–237. https://doi.org/10.1016/j.arabjc.2015.04.027.
[26] A. Kumar, G. Pandey, The photocatalytic degradation of methyl green in presence of visible light with photoactive Ni 0.10: La 0.05: TiO_2 nanocomposites, IOSR Journal of Applied Chemistry 10 (2017), 31–44. https://doi.org/10.9790/5736-1009013144.